IMPROVEMENT OF AERODYNAMIC PERFORMANCE PREDICTION OF HAWT ROTOR BLADES BY A CROSSFLOW TURBULENCE TRANSITION MODEL

Choi J.H. and Kwon O.J.*
Department of Aerospace Engineering,
Korea Advanced Institute of Science and Technology,
Daejeon, 305-701,
Korea,
E-mail: ojkwon@kaist.ac.kr

ABSTRACT

In the present study, an improved laminar-turbulence transition model $\gamma - \widetilde{\mathrm{Re}}_{\theta t} - \mathrm{CF}^{+}$ has been developed for simulating three-dimensional flow transition, including the effect of interaction between the Tollmien-Schlichting and crossflow instabilities. To accommodate the acceleration of the transition process due to the interaction between the two instabilities, a new trigger function was additionally introduced to include the effect of the crossflow instability. Since the main modification was made only in the trigger function, the present model primarily works on local flow variables, and thus can be effectively implemented in the CFD flow solvers based on unstructured meshes by inheriting the advantages of the baseline $\gamma - \widetilde{\mathrm{Re}}_{\theta t}$ transition model. For the validations, the present $\gamma - \widetilde{\mathrm{Re}}_{\theta t} - \mathrm{CF}^{+}$ transition model was applied to the NREL Phase VI wind turbine rotor blade. It was found that the present model is well established, and is useful for predicting the flows involving three-dimensional laminar-turbulence transition more accurately than the $\gamma - \widetilde{\mathrm{Re}}_{\theta t}$ model for simulating horizontal axis wind turbine rotor blade problems.

INTRODUCTION

In modern computational fluid dynamics (CFD), predicting laminar-turbulence transition is one of the most important issues. This is particularly true for general complex three-dimensional configurations, since transition phenomena are closely coupled with complicated three-dimensional flow characteristics. Because general three-dimensional laminar-turbulence transition phenomena are induced mostly by either the Tollmien-Schlichting instability, the crossflow instability, or the interaction of both, it is important to properly capture the effect of those instabilities in simulating general three-dimentional flows.

Recently, the flow solvers based on unstructured meshes are frequently adopted for solving many practical engineering flow problems. In this situation, the problem becomes particularly demanding, because flow transition need to be assessed based only on local flow quantities without relying on the mesh distribution. To predict laminar-turbulence transition using unstructured meshes, a correlation-based transition model, which is called the γ-$\widetilde{\mathrm{Re}}_{\theta t}$ transition model, was first proposed by Langtry and Menter [1]. In their transition model, only local quantities are used in determining the onset of transition. Because of this advantage, the γ-$\widetilde{\mathrm{Re}}_{\theta t}$ model has been used successfully in general-purpose CFD flow solvers for predicting flows accompanying laminar-turbulent transition. However, the γ-$\widetilde{\mathrm{Re}}_{\theta t}$ model has a limited capability for capturing general three-dimensional transition phenomena involving crossflow instabilities, because the Reynolds-number correlation was driven based on the two-dimensional Blasius boundary-layer velocity profiles. A previous study [2] showed that the γ-$\widetilde{\mathrm{Re}}_{\theta t}$ model fails to capture flow transition induced by the crossflow instability.

To overcome this limitation, Choi and Kwon [3] proposed a novel methodology of predicting crossflow-induced transition inside general three-dimensional boundary layers by adopting local flow variables based on the FSC velocity profiles, and suggested a new laminar-turbulence transition model, called γ-$\widetilde{\mathrm{Re}}_{\theta t}$-CF model. Nevertheless, this new transition γ-$\widetilde{\mathrm{Re}}_{\theta t}$-CF model still has a shortcoming that the important interaction phenomena between the Tollmien-Schlichting instability and the crossflow instability are not properly incorporated. This is because implementation of the model was based on the assumption [4] that, when an empirical criterion is utilized for predicting three-dimensional transition phenomena, turbulence appears by either the Tollmien-Schlichting instability or the crossflow instability. However, in real physics, there exists an interaction between the two instabilities, which further accelerates the transition process. Therefore, it is important to develop a transition model which also enables capturing the interaction phenomena.

In the present study, an improved laminar-turbulence transition model γ-$\widetilde{\mathrm{Re}}_{\theta t}$-$\mathrm{CF}^{+}$ has been developed for simulating three-dimensional transition phenomena including the effect of the interaction between the Tollmien-Schlichting and crossflow instabilities. For this purpose, the existing γ-$\widetilde{\mathrm{Re}}_{\theta t}$-CF model [3] was further extended by adopting the e^{N} method's approach [5] which handles the interaction between the two instabilities. For validation, an application was made to the NREL Phase VI wind turbine rotor blades. The results were compared with experimental data and other predictions.

NUMERICAL METHOD

In the present study, based on the same assumption [5] that the transition process is accelerated when both the Tollmien-Schlichting and crossflow instabilities are simultaneously excited, a new turbulence transition model, γ-$\widetilde{Re}_{\theta t}$-CF^{+}, is proposed by introducing a modified form of the function F_{onset1_3D} modification into the γ-$\widetilde{Re}_{\theta t}$-CF transition model [3]. To determine that the transition criteria are fulfilled, the function can be written as:

$$F_{onset1\_3D} = \max\left(F_{onset1}, F_{onset1\_CF}, F_{onset1\_inter}\right)$$

$$F_{onset1\_inter} = \begin{cases} \frac{34}{37}\cdot F_{onset1} + \frac{20}{37}\cdot F_{onset1\_CF}, & F_{onset1} > 0.5 \text{ and } F_{onset1\_CF} > 0.15 \\ 0, & F_{onset1} \le 0.5 \text{ or } F_{onset1\_CF} \le 0.15 \end{cases}$$

Here, F_{onset1_inter}, which is the linear combination of F_{onset1} and F_{onset1_CF}, activates F_{onset1_3D} when the value exceeds one, even though each of the transition criteria, F_{onset1} or F_{onset1_CF}, remains less than one. Through this mechanism, F_{onset1_inter} enables to incorporate the effect of interaction between the Tollmien-Schlichting and crossflow instabilities. The transition criterion considering the interaction between the two instabilities is illustrated in Fig. 1.

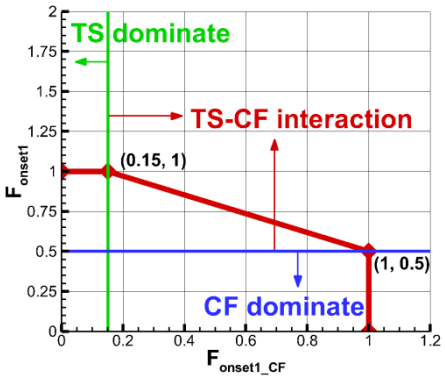

Fig. 1 Illustration of transition criterion considering interaction between Tollmien-Schlichting and crossflow instabilities.

Another modification adopted in the present γ-$\widetilde{Re}_{\theta t}$-CF^{+} model is that the trigger function F_{onset1_CF} in the crossflow direction is now expressed in terms of the critical Reynolds number, $Re_{\delta 2c}$, instead of the transition onset Reynolds number, $Re^{*}_{\delta 2t}$, similar to the streamwise trigger function F_{onset1} :

$$F_{onset1\_CF} = \frac{Re_{v,cross}}{r \cdot Re_{\delta 2c}};\ Re_{\delta 2c} = 0.9 \cdot Re^{*}_{\delta 2t}$$

For the present formulation, F_{lengh_3D} should also be newly estimated. In the present study, F_{lengh_3D} is calibrated by using the experimental data for an inclined 6:1 prolate spheroid at a Reynolds number of 7.2×10^{6} and an angle of attack of 30 degrees [6] as:

$$F_{length\_3D} = \begin{cases} \left[398.189\cdot10^{-1} - \left(119.270\cdot10^{-4}\right)Re_{CF} - \left(132.567\cdot10^{-6}\right)Re_{CF}^{2}\right], & Re_{CF} < 400 \\ \left[263.404 - \left(123.939\cdot10^{-2}\right)Re_{CF} + \left(194.548\cdot10^{-5}\right)Re_{CF}^{2} - \left(101.695\cdot10^{-8}\right)Re_{CF}^{3}\right], & 400 \le Re_{CF} < 596 \\ \left[0.5 - \left(Re_{CF} - 596\right)\cdot3.0\cdot10^{-4}\right], & 596 \le Re_{CF} < 1200 \\ [0.3188], & 1200 \le \widetilde{Re_{CF}} \end{cases}$$

$$Re_{CF} \equiv Re_{\theta t}\left(1 - \frac{\phi}{\pi/2}\right)$$

Here, the effect of crossflow instability is implemented by the term $\left(1\text{-}\frac{\phi}{\pi/2}\right)$, and, as a result, F_{lengh_3D} returns to its original form, F_{lengh}, when the local sweep angle, ϕ, approaches zero.

More detailed information about the present transition model can be found in Ref. [7].

RESULTS AND DISCUSSION

To investigate the practical applicability of the present γ-$\widetilde{Re}_{\theta t}$-CF^{+} model to rotating bodies, calculations were made for the upwind axial flow cases of the NREL Phase VI wind turbine rotor blades, and the results are compared with those of the experiment [8] and other predictions [2]. The measurements were made at a rotational speed of 71.63rpm, and the inflow wind speed varied from 7m/s to 25m/s. The calculations were also made by using the fully-turbulent k-ω SST model, the baseline γ-$\widetilde{Re}_{\theta t}$ transition model [1], and the γ-$\widetilde{Re}_{\theta t}$-CF transition model [3] for comparison. It was reported in the previous study [2] that, for this particular wind turbine configuration, laminar-turbulent transition mainly influences the rotor aerodynamic performances at inflow wind speeds of 10m/s to 15m/s. In the calculations, the freestream turbulent intensity, Tu_{FS}, was set to 0.5%, and the viscosity ratio, $(\mu_T/\mu)_{FS}$, was set to five.

In Fig. 2, the computational domain and the imposed boundary conditions are presented. To eliminate the effect of boundary condition, the downstream boundary was set at 15 rotor radii downstream from the rotor disc plane. At the upstream boundary located six rotor radii from the rotor, an inflow condition was imposed. In the radial direction, the side boundary was set at 3.5 rotor radii away from the rotor shaft axis. For this two-bladed rotor, the calculations were made only for a single blade by imposing a periodic boundary between the blades. The unstructured hybrid mesh consisted of 6,683,329 cells, 2,777,943 nodes, and 145,330 boundary faces. To capture the boundary layer accurately, 35 prism layers are packed on the blade surface. The initial thickness of the prism cell is 1.11×10^{-5}R, and the y^{+} value at the first prism layer is approximately 0.5.

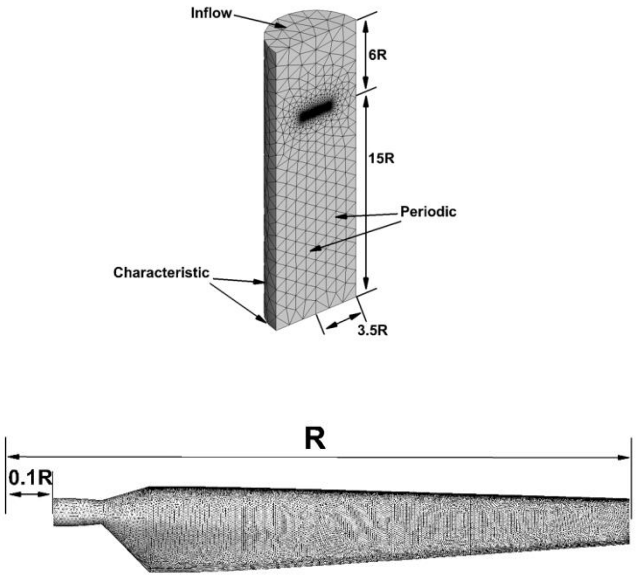

Fig. 2 Computational domain and boundary condition for NREL Phase VI rotor blades.

In Fig. 3, the predicted shaft torque distributions of the NREL Phase VI rotor for different inflow wind speeds are compared between different turbulence models. It is shown that, in the case of the inflow wind speed of 7, 20, and 25 m/s, the fully-turbulent model and all transition models predict similar shaft torques, because at these inflow conditions the laminar-turbulent transition has no direct effects on the rotor as reported in the previous study [2]. However, in the case of three transient inflow wind speeds of 10, 13, and 15 m/s, a fairly large difference is observed between the models. The fully-turbulent k-ω SST model overpredicts the shaft torque because the model does not capture the laminar flow region, while the baseline γ-$\widetilde{Re}_{\theta t}$ transition model underpredicts because it fails to capture the transition induced by crossflow instability. This underprediction of the γ-$\widetilde{Re}_{\theta t}$ transition model is also observed in Sørensen's result [2], except at the inflow wind speed of 10m/s. In contrast, both the γ-$\widetilde{Re}_{\theta t}$-CF and γ-$\widetilde{Re}_{\theta t}$-$CF^{+}$ models capture the transition due to crossflow instability, and predict the shaft torque more accurately than the other models, even though there exists some deviation from the experimental data at 15m/s inflow wind speed. In the present case, it is shown that the transition of the rotor mainly induced by the crossflow instability because the difference between the γ-$\widetilde{Re}_{\theta t}$-CF and γ-$\widetilde{Re}_{\theta t}$-$CF^{+}$ model is almost negligible.

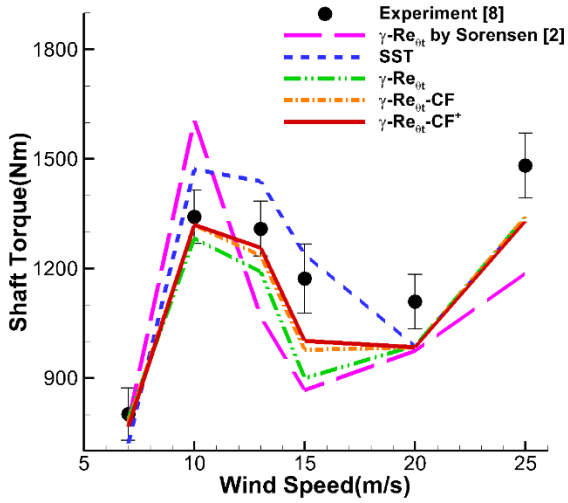

Fig. 3 Predicted shaft torque of NREL Phase VI rotor.

In Fig. 4, the radial variations of the normal and tangential force coefficients are compared between the fully-turbulent model and the transition models. The measurements were made at five selected spanwise locations (0.3, 0.47, 0.63, 0.8, and 0.95 R). The results again confirm that the present transition model works well by capturing the transition due to crossflow instability. In the case of tangential force coefficient, it is shown that the present γ-$\widetilde{Re}_{\theta t}$-$CF^{+}$ model predicts the coefficient more accurately than the other models, particularly at 0.63 R section for the 10m/s inflow case, 0.8 R section for the 13m/s inflow case, and 0.95 R section for the 15m/s inflow case. This is because the transitional regions move radially towards the rotor blade tip as the inflow wind speed is increased. In the case of normal force coefficient, the difference between the fully-turbulent model and the transition models becomes smaller than the tangential force coefficient, because the laminar-turbulent transition mainly influences the skin friction force rather than pressure force. Nevertheless, the present γ-$\widetilde{Re}_{\theta t}$-$CF^{+}$ model shows better results in normal force also, especially, at the inflow wind speed of 15m/s. The present transition model compares better than the fully-turbulent k-ω SST model for the 0.8 R section and also than the baseline γ-$\widetilde{Re}_{\theta t}$ model for the 0.95 R section.

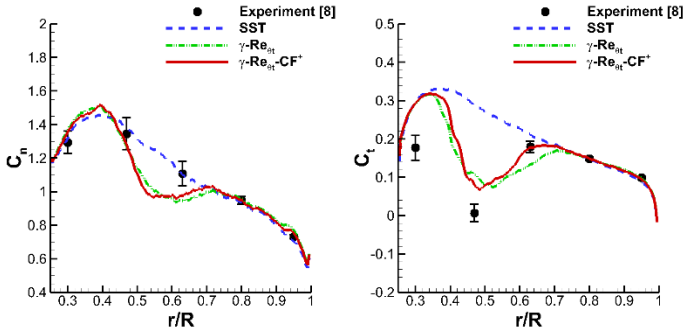

(a) Inflow wind speed of 10m/s

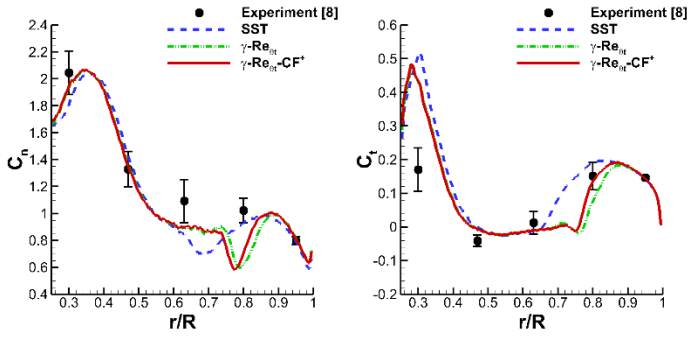

(b) Inflow wind speed of 13m/s

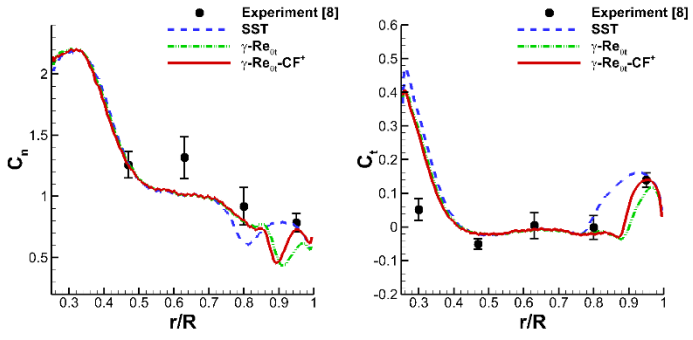

(c) Inflow wind speed of 15m/s

Fig. 4 Comparison of radial variations of normal and tangential force coefficients for NREL Phase VI rotor at three inflow wind speed of 10, 13, and 15 m/s.

CONCLUSIONS

In the present study, an improved laminar-turbulence transition model γ-$\widetilde{Re}_{\theta t}$-CF$^+$ has been developed for simulating three-dimensional transition including the effect of interaction between the Tollmien-Schlichting and crossflow instabilities. For this purpose, a new trigger function, F_{onset1_inter}, is introduced into the previously proposed γ-$\widetilde{Re}_{\theta t}$-CF model to consider the acceleration of the transition process due to the interaction between the two instabilities. Because the main modification in the present γ-$\widetilde{Re}_{\theta t}$-CF$^+$ model lies in the trigger function, the present model works on local flow variables, and thus can be effectively implemented in CFD solvers based on unstructured meshes by inheriting the advantages of the baseline γ-$\widetilde{Re}_{\theta t}$ transition model,.

For validation, the present γ-$\widetilde{Re}_{\theta t}$-CF$^+$ model was applied to the NREL Phase VI wind turbine rotor blades. It was shown that the γ-$\widetilde{Re}_{\theta t}$-CF and γ-$\widetilde{Re}_{\theta t}$-CF$^+$ model capture the transition due to crossflow instability, and predict the shaft torque more accurately. Also, it was observed that flow transition on the rotor blades mainly is mainly induced by the crossflow instability because the difference between the γ-$\widetilde{Re}_{\theta t}$-CF and γ-$\widetilde{Re}_{\theta t}$-CF$^+$ model is almost negligible.

ACKNOWLEDGEMENT

This work was supported by the New & Renewable Energy Core Technology Program of the Korea Institute of Energy Technology Evaluation and Planning (KETEP), granted financial resource from the Ministry of Trade, Industry & Energy, Republic of Korea (No. 20153030023880). This research was also supported by the Climate Change Research Hub of KAIST (Grant No. N01150026).

REFERENCES

[1] Langtry, R. B., and Menter, F. R., "Correlation-Based Transition Modeling for Unstructured Parallelized Computational Fluid Dynamics Codes," AIAA Journal, Vol. 47, No. 12, 2009, pp. 2894-2906.

[2] Sørensen, N. N., "CFD Modelling of Laminar-turbulent Transition for Airfoils and Rotors Using the γ-$\widetilde{Re}_{\theta t}$ Model," *Wind Energy*, Vol. 12, No. 8, 2009, pp. 715-733.

[3] Choi, J. H., and Kwon, O. J., "Enhancement of a Correlation-Based Transition Turbulence Model for Simulating Crossflow Instability," AIAA 2014-1133, *52th AIAA Aerospace Sciences Meeting*, National Harbor, Maryland, 2014.

[4] Arnal, D., Casalis, G., and Houdeville, R., "Practical Transition Prediction Methods: Subsonic and Transonic Flows," VKI Lectures Series *Advances in Laminar-Turbulent Transition Modeling*, 2008. Also ONERA RF 1/13639 DMAE, September 2008.

[5] Stock, H. W., "e^N Transition Prediction in Three-Dimensional Boundary Layers on Inclined Prolate Spheroids," *AIAA Journal*, Vol. 44, No. 1, 2006, pp. 108-118.

[6] Kreplin, H. P., Vollmers, H., and Meier, H. U., "Wall Shear Stress Measurements on an Inclined Prolate Spheroid in the DFVLR 3M×3M Low Speed Wind Tunnel, Göttingen," DFVLR-AVA, Rept. IB 222-84 A 33, Göttingen, Germany, 1985.

[7] Choi, J. H., and Kwon, O. J., "Recent Improvement of a Correlation-Based Transition Turbulence Model for Simulating Three-Dimensional Boundary Layers," Presented at the 22nd AIAA Computational Fluid Dynamics Conference, June. 22-26, 2015, Dallas, Texas, AIAA Paper 2015-2762.

[8] Hand, M. M., Simms, D. A., Fingersh, L. J., Jager, D. W., Cotrell, J. R., Schreck, S., and Larwood, S. M., "Unsteady Aerodynamics Experiment Phase VI: Wind Tunnel Test Configurations and Available Data Campaigns." NREL, TP-500-29955, 2001.